Functionalization of single-walled carbon nanotubes using isotropic plasma treatment: Resonant Raman spectroscopy study

Zhandos N. Utegulov[a] and David B. Mast
Department of Physics, University of Cincinnati, Cincinnati, Ohio 45221

Peng He and Donglu Shi
Department of Chemical and Materials Engineering, University of Cincinnati, Cincinnati, Ohio 45221

Robert F. Gilland
Department of Electrical and Computer Engineering and Computer Science, University of Cincinnati, Cincinnati, Ohio 45221

(Received 18 November 2004; accepted 22 March 2005; published online 10 May 2005)

Functionalization of single-walled carbon nanotubes (SWNTs) by isotropic plasma treatment was studied using resonant Raman spectroscopy. It was shown that plasma-induced functionalization results in the uniaxial isotropic constriction of the nanotubes but preserves their overall structural integrity. It was demonstrated that $NH_3 \cdot H_2O$ and hexamethyldisiloxan plasmas yield various types of conductivity for semiconducting SWNTs. © *2005 American Institute of Physics*.
[DOI: 10.1063/1.1913801]

I. INTRODUCTION

Single-walled carbon nanotubes (SWNTs) have been at the forefront of nanoscale investigations due to their unique structure-dependent electronic, optical and mechanical properties.[1] They are thought to have a host of wide-ranging, potential applications, for example, as catalyst supports in heterogeneous catalysis, field emitters, high strength engineering fibers, sensors, actuators, tips for scanning probe microscopy, gas storage media, and as molecular wires for the next generation of electronics and optoelectronics devices.[2–4]

To realize many of these nanotube-based devices, the surface modification or functionalization of carbon nanotubes has to be achieved while largely retaining their structural integrity. Surface-functionalized SWNTs are chemically more reactive than bare nanotubes and therefore can be employed for further processing and integration as for example in nanocomposites.[5] Whereas the chemistry of fullerenes is well-established, the chemistry of SWNTs is relatively an unexplored field of research. The bonding of the chemical functional groups to the walls of the carbon nanotubes is a very important area of study because it provides fundamental understanding on how nanoscale interactions occur with the potential to substantially enhance the intrinsic properties of SWNTs.

The traditional approach to modify the properties of pristine SWNTs is to use wet chemistry and/or exposure to high-temperature vapors. The high-temperature approach may damage the nanotubes depending on temperature and exposure to air during processing. In addition, certain chemistries may not be accessible in the vapor phase. Wet chemistry in large scale may lead to waste disposal, and in general, involves several additional steps, such as dissolution, sonication, mixing, drying, etc. Besides, this process can yield undesirable agglomeration of treated particles. The alternative to these methods is *plasma-induced treatment and polymerization*.

There have been several works recently devoted to the study of the effect of plasma treatment on the surface of SWNTs.[6–12] Plasma polymerization is an environmentally friendly, solvent-free, and time efficient thin-film-forming process with room-temperature processing ability to produce plasma polymer composites on a large scale. Therefore, the plasma-induced functionalization method is believed to be superior compared to a chemical method. Plasma treatment has been widely used for surface activation of various materials, ranging from organic polymers to inorganic ceramics and metals.[13] During plasma treatment the radio frequency (rf) glow discharge is formed when gaseous monomers are subjected to a rf electrical field at a relatively low pressure. During the glow-discharge process, excited electrons, ions, and free radicals are generated through inelastic collisions between energetic electrons and molecules. The plasma species thus formed are very reactive toward surfaces, leading to surface modification. It should be also noted that the plasma-induced deposited films consisting of functional groups[7] or polymer[9] are on the nanoscale size.

During plasma treatment of carbon nanotubes, mentioned above, several plasma chemicals were used, e.g., acetaldehyde,[6] CO_2,[7] H_2,[10,11] F_2,[12] O_2,[14] and CF_4,[12] resulting in the formation of high polarity of the carbon nanotubes (CNT) surface and improved overall adhesion of CNTs to the surrounding polymer matrix. Our preliminary results on Raman spectra of CNTs plasma coated with ultrathin polystyrene polymer[15] showed substantial covalent bonding of the polymer to the tubes and unwrapping of SWNT bundles, thus allowing for more uniform dispersion of the CNT in the composite. The technique similar to plasma treatment, called ion-beam modification, has also been used to modify the properties of carbon nanotubes[16,17] and it was shown, like in plasma method, that the ion-beam-induced modifications

[a]Electronic mail: utegulov@physics.uc.edu

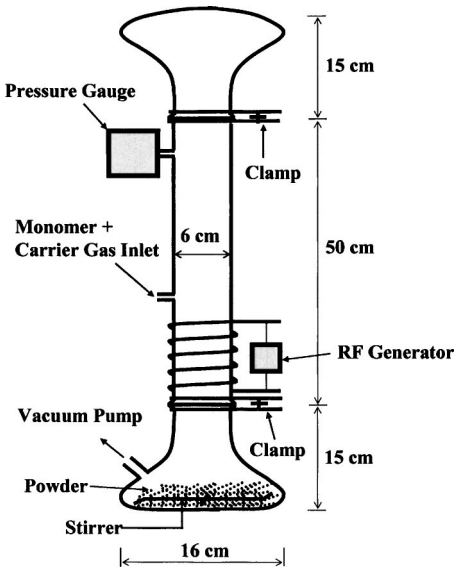

FIG. 1. Plasma reactor used for isotropic plasma treatment of carbon nanotubes.

produces cross-links between otherwise unfunctionalized nanotubes and polymer backbone chains that serve to toughen the composite.

In this paper we demonstrate the clean and room-temperature plasma-induced functionalization of SWNTs by activating plasma, varying plasma power levels, and introducing various plasma monomers like ammonia and organosilicon compound called hexamethyldisiloxan (HMDSO). Unpolarized resonant Raman spectroscopy is used to analyze the result of plasma functionalization on SWNT structure.

II. EXPERIMENT

Purified pristine HiPCO SWNTs were supplied by Carbon Nanotechnologies Inc. The vacuum chamber of the plasma reactor consists of a Pyrex glass column 80 cm in height and 6 cm in internal diameter (see Fig. 1). The pure nanotubes were vigorously stirred at the bottom of the reactor so that their surface is continuously renewed by the stirrer and exposed to the plasma for isotropic thin-film deposition. A magnetic bar was used to stir the powders. The monomers were introduced from the gas inlet during plasma treatment process. The system pressure was measured by a thermocouple pressure gauge. A discharge by rf signal of 13.56 MHz was used for the plasma film deposition. Before the plasma treatment, the base pressure was pumped down to less than 30 mTorr before the monomer vapors were introduced into the reactor chamber. The operating pressure was adjusted by the mass flow controller. The pristine SWNT sample is labeled as sample 1. Samples 2 and 3 are the plasma-treated SWNTs with no introduction of any monomer at 10 and 100 W respectively. In both cases the total pressure in the plasma reactor was 30 mTorr. Sample 4 contains SWNTs plasma treated by the $NH_3 \cdot H_2O$ monomer introduced into the reactor for a total pressure of 200 mTorr and rf power of 30 W. For sample 5 the monomer was changed to HMDSO, organic silicon compound $[(CH_3)_3SiOSi(CH_3)_3]$, with the other processing parameters held the same. For all four-functionalized SWNT samples, the processing time was kept constant at 30 min.

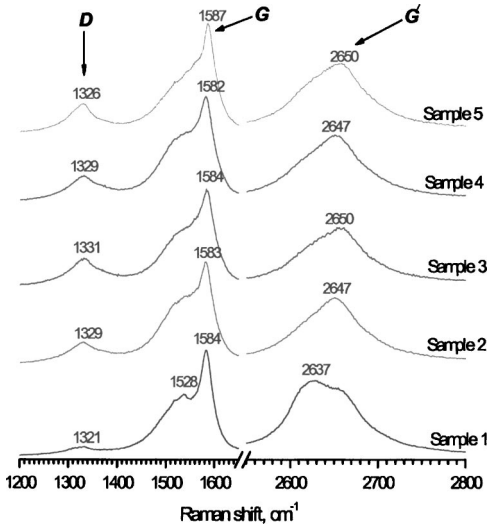

FIG. 2. Raman spectra of the *D*, *G*, and *G′* bands for the pristine- and plasma-treated SWNTs.

The resonant Raman spectra were measured in the backscattering geometry using Renishaw inVia Raman spectrometer equipped with an Olympus microscope with the 50× objective to focus 514.5-nm Ar^+ ion laser beam on the sample. The Raman results for the pristine and plasma-treated SWNTs are shown in Figs. 2 and 3.

III. RESULTS AND DISCUSSION

The Raman scattering spectra from all four plasma-treated samples (samples 2–5) in Fig. 2 clearly show the typical resonant Raman peaks inherent for SWNTs, e.g., low-frequency radial breathing mode (RBM) peaks and double-peak structure just below 1600 cm^{-1} called *G*-band, attributable to tangential stretching C–C mode vibrations. Therefore, the nanotubes structural integrity is preserved under all plasma conditions. The diameter values d(nm) for pristine-

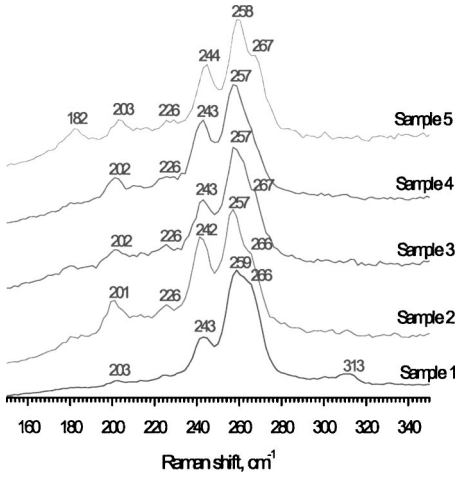

FIG. 3. Raman spectra of the RBM modes for pristine- and plasma-treated SWNTs.

and plasma-treated SWNTs are estimated to be in the 0.74–1.35-nm range using phenomenological power law:[18] $d(\mathrm{nm})=[238/\nu(\mathrm{cm}^{-1})]^{1.075}$.

For samples 2 and 3 before turning the plasma on, we have a monomer-free situation where there are only the essential components of the air under small base pressure of 30 mTorr present in the plasma reactor. These components are oxygens (21%), nitrogen (78%), and 1% of CO_2, H_2, He, Ar, etc. By turning the plasma on, we effectively dissociate the oxygen molecules: $O_2=2O$. In this case the oxygen [O] atoms have much higher tendency to react with carbon atoms of SWNT than nitrogens [N] do, despite of much lower concentration of molecular O_2 with respect to that of N_2, because nitrogen dissociation energy is higher than that of the oxygen.[19] Since the main structural backbone of the SWNT is preserved, therefore, we expect the functionalization of the tubes in this case to be accompanied primarily by *oxidation* process. It should be noted that the concentration of dissociated oxygens increases with the increasing power in the low power range, therefore sample 3 is expected to have higher degree of oxygen containing functional groups attached to the walls of SWNTs than sample 2. The previous x-ray photoelectron spectroscopy (XPS) characterization of the uppermost layer of oxygen plasma-treated carbon nanotubes showed that the layers mainly consisted of carbonyl (C═O), hydroxide (C–OH) and carboxyl (COOH) groups.[7]

Plasma dissociation of ammonia $NH_3 \cdot H_2O$ monomer most likely results in the appearance of $C-NH_2$ groups due to $NH_3 \rightarrow NH_2+H$ reaction and the formation of C–OH groups due to $H_2O \rightarrow OH+H$ reaction. It should be noted that the plasma activation in this case would result in much larger number of $C-NH_2$ and C–OH functional groups compared to the amount of oxygen containing groups attached to the walls of the nanotubes because the dissociation energy of ammonia and water is much lower than that of oxygen and nitrogen. Thus, the degree of functionalization is expected to be stronger for the sample 4 than for the monomer-free samples 2 and 3. Recent functionalization of SWNTs by ammonia microwave glow-discharge yielded NH_2, NH, H, and N radicals, all of which are able to bond to the nanotube walls.[20]

Plasma treatment of the SWNT surface with HMDSO would most likely result in the formation of the *polymer* film on the surface of the nanotubes. The *polymerization* around the surface of the nanotubes will possibly be due to involvement of such backbone atoms as Si and C. Oxygen and hydrogen will have small chance to be associated with the polymerization process because of their small valence. Due to plasma exposure the HMDSO molecule would undergo dissociation and be deposited in the form of mostly $Si-CH_3$ functional groups, which is supported by early XPS surface analysis of HMDSO plasma deposits[21] and Si doping in fullerenes.[22] Once the Si atom is inserted in the SWNT, the binding of other elements to it will be very strong.[23,24] This is a very attractive property, since most atoms and molecules that have recently been shown to alter the electronic properties of SWNTs (e.g., O_2) adsorb only weakly on tubes. In particular, the half-occupied energy level of the $Si-CH_3$ complex is 0.219 eV above the top of the nanotubes valence band.[25] This energy level characterizes this chemical complex as deep acceptor in the semiconducting SWNT.

The *G*-band, attributable to the tangential mode (TM) C–C stretching vibrations, for the sample 1 has double-peak structure typical for the SWNTs as shown in Fig. 2. Low-frequency ($1528\ \mathrm{cm}^{-1}$) and high-frequency ($1584\ \mathrm{cm}^{-1}$) components of the TM are associated with vibrations along the circumferential and nanotubes axis directions, respectively. The fact that the peak at $1584\ \mathrm{cm}^{-1}$ is stronger than that at $1528\ \mathrm{cm}^{-1}$ for all Raman spectra implies that we probe the predominantly semiconducting nanotubes. With the plasma exposure the shoulder at $1528\ \mathrm{cm}^{-1}$ becomes less resolved, but the ratio of its height to that of 1583-cm^{-1} peak remains constant for all samples suggesting that predominantly semiconducting tubes are probed for all samples. The lower-frequency tail of the TM is usually described by the Breit-Wigner-Fano (BWF) lineshape function which is associated with the resonance involving interference between the Raman scattering from continuum excitations and that from a discrete phonon, provided the two Raman-active excitations are coupled.[26] The degree of coupling determines the departure of the lineshape from symmetric Lorentzian function. The metallic contribution to the overall conductivity of the tubes described by the BWF peak is small for both the pristine and plasma treated samples. For the nanotubes sample exposed to ammonia plasma (sample 4) we observe the decrease in the frequency of the TM from 1584 down to $1582\ \mathrm{cm}^{-1}$. Similar frequency downshift was observed in case of microwave ammonia plasma treatment of SWNTs.[27] As stated above, plasma dissociation of ammonia would result in the abundance of $C-NH_2$ bonds. The negatively charged NH_2 terminal can be also used as a stable electron donor. The downward shift of the TM as was observed in[27,28] points out to the electron doping in NH_2-terminated samples.[28] The softening of this mode can be interpreted in terms of valence electron transfer from an electron donor, the amine group, into the carbon π^* band,[29] resembling graphite intercalation compounds. On the contrary, its stiffening was observed upon the doping with electron acceptors. The latter result can be seen in the case of nanotubes exposure to HMDSO plasma (sample 5): the TM's frequency increases from 1584 up to $1587\ \mathrm{cm}^{-1}$. These results are supported by the formation of the $Si-CH_3$ acceptor discussed above and are in general agreement with the observed sensitivity of the several vibrational modes of SWNTs to doping processes,[29] reflecting the increase or decrease of the C–C bond-bending and bond-stretching force constants resulting from the charge transfer, intercalation, and controlling the position of the Fermi level (E_F).[30,31] We also show that monomer-free plasma activation does not affect the frequency of the LO tangential mode at both 10 and 100 W, implying that there is no shift in the type of semiconducting conductivity.

All plasma exposed SWNTs (i.e., samples 2–5) have gained more disordered sp^3 bonds associated with the *functionalization* compared to the pristine nanotubes sample 1, as evidenced from the enhancement of the *D*-band's height. Both, the *D* ($1321\ \mathrm{cm}^{-1}$) and second-order *G′* ($2637\ \mathrm{cm}^{-1}$) bands shift to higher wave numbers as shown in Fig. 2. The upshift of the *D*-band's frequency is attributed to the harden-

ing of the C–C bond due to nanotubes curvature[32] caused by plasma exposure. The presence of the G'-band does not depend on defects, but is sensitive to the strain. This peak is very intense and easily observable in the Raman spectra. It is known that the hydrostatic pressure causes the increase in the wave number of the G' band[33–35] which can be found for any form of compressive deformation such as when the nanotubes are deformed inside a composite. However, this type of pressure also causes the increase in the wave number of the RBMs (Ref. 36) which is *not* found in our results as shown in Fig. 3. Thus, we rule out the possibility of the plasma induced *hydrostatic* compression. In the RBM range we observe the plasma-induced relative height enhancement of the lower-frequency RBM modes at 182, 203, 226, 243, and 259 cm^{-1} along with the suppression of the higher-energy RBM modes at 266 and 313 cm^{-1}, suggestive of the effective damping for the Raman activity for the small diameter tubes. With the increase of driving power from 10 to 100 W as seen for samples 2 and 3, the Raman bands at 226 and 259 cm^{-1} become pronounced. The enhancement of the breathing mode bands occur probably because the functional groups attached to the sidewalls improve the radial breathing oscillation upon plasma-induced oxidation. Exactly the same effect of the Raman intensity variation for the breathing modes as they go in and out of resonance with no shift in the RBM band positions have been recently found in the *uniaxialy* compressed nanotubes in the epoxy/SWNT composites.[37] The exertion of the uniaxial constriction on our tubes can take place as a result of the *isotropic* plasma exposure due to continuous renewal of the plasma reactor's stirrer. Besides, there is the wave-number upshift of the G' band from 2647 to 2650 cm^{-1} as shown for samples 2 and 3, i.e., as the plasma-driving power increases from 10 to 100 W. This trend provides an evidence that the enhanced nanotubes oxidation, activated by the increase in the plasma power, causes SWNTs to be more uniaxially compressed.

IV. CONCLUSION

Isotropic plasma treatment was shown to be effective tool to functionalize SWNTs. The Raman results show that the plasma-treated nanotubes have retained overall structural integrity in spite of the uniaxial constriction resulted after plasma exposure, as the driving power is increased for the monomer-free plasma, as the plasma monomer is introduced and the type of monomer is changed from ammonia to HMDSO. It was demonstrated that the ammonia and HMDSO plasma treatments facilitate the formation of *n*- and *p*-type semiconducting nanotubes, respectively. However, the increase in the monomer-free plasma driving power did not result in the shift of the conductivity type. We strongly believe in the usefulness of isotropic plasma treatment method as a potential for producing materials with controllable physicochemical properties and desirable features to be attractive for nanotubes-based device applications. The XPS study will be needed for a detailed structural elucidation of various functional groups attached to the walls of the carbon nanotubes after plasma treatment.

ACKNOWLEDGMENTS

This work is supported in part by AFRL Contract No. F33615-02-C-5704. We thank John Busbee and Jason Reber of AFRL/MLMT and John Maguire of AFRL/MLBP, Write-Patterson Air Force Base for assistance in taking the Raman spectra.

[1] M. S. Dresselhaus, G. Dresselhaus, and P. Avouris, *Carbon Nanotubes. Synthesis, Structure, Properties and Applications* (Springer, Berlin, 2001).
[2] P. Avouris and J. Appenzeller, Ind. Phys. **10(3)**, 18 (2004).
[3] A. Bachtold, P. Hadley, T. Nakanshi, and C. Dekker, Science **294**, 1317 (2001).
[4] R. H. Baughman, A. A. Zakhidov, and W. A. de Heer, Science **297**, 787 (2002).
[5] Y.-P. Sun, K. Fu, Y. Lin, and W. Huang, Acc. Chem. Res. **35**, 096 (2002).
[6] Q. Chen, L. Dai, M. Gao, S. Huag, and A. Mau, J. Phys. Chem. B **105**, 618 (2001).
[7] H. Bubert, S. Haiber, W. Brandl, G. Marginean, M. Heintze, and V. Bruser, Diamond Relat. Mater. **12**, 811 (2003).
[8] L. Dai, Radiat. Phys. Chem. **62**, 55 (2001).
[9] D. Shi, J. Lian, P. He, L. M. Wang, W. J. van Ooij, M. Schulz, Y. Liu, and D. B. Mast, Appl. Phys. Lett. **81(27)**, 5216 (2002).
[10] B. N. Khare, M. Meyyappan, A. M. Cassel, C. V. Nguen, and J. Han, Nano Lett. **2**, 74 (2002).
[11] B. N. Khare, M. Meyyappan, J. Kralj, P. Wilhite, M. Sisay, H. Imanaka, J. Koehne, and C. W. Baushchilcher, Appl. Phys. Lett. **81**, 5237 (2002).
[12] N. O. V. Plank, L. Jiang, and R. Cheung, Appl. Phys. Lett. **83(12)**, 2426 (2003).
[13] L. Dai, J. Macromol. Sci., Rev. Macromol. Chem. Phys. **39**, 237 (1999).
[14] C. U. Pittman, Jr, W. Jiang, G.-R. He, and S. D. Gardner, Carbon **36(1–2)**, 25 (1998).
[15] D. Mast, R. Gilliland, Z. Utegulov, P. He, M. J. Schulz, Y. Liu, D. Shi, and W. J. van Ooij, Deposition of Extremely Thin Polymer Films on Carbon Nanotube Surfaces by a Plasma Treatment, NanoMaterials for Defense Applications Symposium, Maui, HI 19–26 February 2004 (unpublished).
[16] B. Ni, R. Andrews, D. Jacques, D. Qian, M. B. J. Wijesundara, Y. Choi, L. Hanley, and S. B. Sinnott, J. Phys. Chem. B **105**, 12719 (2001).
[17] Y. Hu and S. B. Sinnot, J. Mater. Chem. **14**, 719 (2004).
[18] J.-L. Sauvajol, E. Anglaret, S. Rols, and L. Alvarez, Carbon **40**, 1697 (2002).
[19] H. Yasuda, *Plasma Polymerization* (Academic, New York, 1985).
[20] Z. Liu, Z. Shen, T. Zgu, S. Hou, and L. Ying, Langmuir **16**, 3569 (2000).
[21] M. R. Alexander, R. D. Short, F. R. Jones, M. Stollenwerk, J. Zabold, and W. Michaeli, J. Mater. Sci. **31**, 1879 (1990).
[22] J. L. Fye and M. F. Jarrold, J. Phys. Chem. A **101**, 1836 (1997).
[23] S. B. Fagan, A. J. R. da Silva, R. Mota, R. J. Baierle, and A. Fazzio, Phys. Rev. B **67**, 033405 (2003).
[24] R. J. Baerle, S. B. Fagan, R. Mota, A. J. R. da Silva, and A. Fazzio, Phys. Rev. B **64**, 085413 (2001).
[25] S. B. Fagan, R. Mota, R. J. Baierle, A. J. R. da Silva, and A. Fazzio, Mater. Charact. **50**, 183 (2003).
[26] P. C. Eklund and K. R. Subbaswamy, Phys. Rev. B **20**, 5157 (1979).
[27] B. N. Khare *et al.*, J. Phys. Chem. **108**, 8166 (2004).
[28] P. W. Chiu, G. S. Suesberg, U. Dettlaf-Weglikowska, and S. Roth, Appl. Phys. Lett. **80(20)**, 3811 (2002).
[29] A. M. Rao, P. C. Elkund, S. Bandow, A. Thess, and R. E. Smalley, Nature (London) **388**, 257 (1997).
[30] P. Petit, C. Mathis, C. Journet, and P. Bernier, Chem. Phys. Lett. **305**, 370 (1990).
[31] E. Jouguelet, C. Mathis, and P. Petit, Chem. Phys. Lett. **318**, 561 (2000).
[32] A. G. Souza Filho, A. Jorio, G. G. Samsonidze, G. Dresselhaus, R. Saito, and M. S. Dresselhaus, Nanotechnology **14**, 1130 (2003).
[33] C. A. Cooper and R. J. Young, J. Raman Spectrosc. **30**, 929 (1999).
[34] P. M. Ajayan, L. S. Schandler, G. Giannaris, and A. Rubio, Adv. Mater. (Weinheim, Ger.) **12**, 750 (2000).
[35] C. A. Cooper, R. J. Young, and M. Halsall, Composites, Part A **32**, 401 (2001).
[36] U. D. Venkateswaran, A. M. Rao, E. Richter, M. Menon, A. Rinzler, R. E. Smalley, and P. C. Eklund, Phys. Rev. B **59**, 10928 (1999).
[37] M. Lucas and R. J. Young, Phys. Rev. B **69**, 085405 (2004).